Available online at www.sciencedirect.com
SCIENCE DIRECT®
Biochimica et Biophysica Acta 1655 (2004) 172–178
BIOCHIMICA ET BIOPHYSICA ACTA
BBA
www.bba-direct.com

Review

Water oxidation in PSII—H atom abstraction revisited

Ron J. Pace[a,*], Karin A. Åhrling[a,b]

[a] Department of Chemistry, Faculty of Science, Australian National University, Building 33, Canberra 0200, Australia
[b] Research School of Biological Sciences, Australian National University, Canberra 0200, Australia

Received 14 March 2003; accepted 1 September 2003

Abstract

A model for the water oxidation reaction in Photosystem II (PSII) is presented, based on an H atom abstraction mechanism. The model rationalises the S-state dependence of observed substrate water exchange kinetics [Biochim. Biophys. Acta 1503 (2001) 197] and assumes that H transfer occurs to an oxidised μ-oxo bridge oxygen on the $S_3 \rightarrow S_4 \rightarrow S_0$ transition. The model requires that only one Mn-pair and a Ca ion be directly involved in the substrate binding and catalytic function. The multiline signal observed in the S_0 state is shown to plausibly arise from such a system. A detailed molecular model of the three-metal site, assuming ligation by those residues identified by mutagenesis as Ca/Mn ligands is presented. This bears a resemblance to the dinuclear Mn site in Mn catalase and is generally consistent with the electron density map of cyanobacterial PSII recently presented [Proc. Natl. Acad. Sci. U. S. A. 100 (2003) 98].

Keywords: Photosystem II; Mn cluster; Water oxidising complex; H atom abstraction

1. Introduction

The structure and mechanism of the Mn-containing water oxidising complex (WOC) in Photosystem II (PSII) remain among the last great challenges in bioenergetics. The Mn/Ca cluster in PSII is the most efficient anodic, 'electrolysis' system known. It operates under mild conditions of temperature, pH, electrolyte background, etc., with a maximum turnover rate $\sim 10^3$/s and an extremely low over-voltage (i.e. activation energy ~ 0.1 eV). Its operation is greatly superior to any conventional electrolytic processes and is close to the absolute thermodynamic limit. But how is this achieved?

An important insight came with the proposal by Babcock, Hoganson, Tommos et al. [1–3] that H abstraction from water (i.e. coupled electron proton transfer) was the key catalytic mechanism employed. This recognised that effectively neutral atom exchange would minimise reorganisation energies, so lowering activation barriers in the overall process. As originally elaborated, the H atom acceptor was the phenoxide oxygen of the redox active tyrosine radical $Y_{\dot{Z}}$ (see appropriate article, this issue). Although mechanistically attractive when first proposed, subsequent developments challenged this position. In particular, at least one transition ($S_1 \rightarrow S_2$) in the S-state turnover of the water oxidising site appears to be electrogenic (not charge neutral) [4]. Further, from the recent structural data on cyanobacterial PSII [5,6], the closest approach of a Mn to the phenoxide oxygen of Y_Z (~ 7 Å) would seem to exclude H transfer from a Mn ligated water/hydroxyl, as originally suggested.

When Ron visited East Lansing in late 1999, he and Jerry discussed what *alternatives* to Y_Z might exist as H atom acceptors in water oxidation. They agreed that the earlier energetic analysis [3] strongly indicated that a *radical*, oxygen centred species would be most likely. Jerry, following William of Occam, favoured Y_Z on the grounds that it was the *known* redox active radical species near the Mn cluster. One other possibility examined was an oxidised bridge oxygen in one of the two di-μ-oxo bridged Mn pairs, identified by extended X-ray absorption fine structure (EXAFS) as the dominant features of the Mn cluster geometry (see Ref. [7]). Such an oxidation was proposed by Yachandra et al. [7] as the basis of the small Mn X-ray absorption near edge spectroscopy (XANES) shift and

Abbreviations: XANES, X-ray absorption near edge spectroscopy; EXAFS, extended X-ray absorption fine structure; MeOH, methanol; WOC, water oxidising complex; PSII, Photosystem II; EPR, electron paramagnetic resonance; NIR, near infrared; ML, multiline; ENDOR, electron nuclear double resonance

* Corresponding author. Tel.: +61-2-6125-4546; fax: +61-2-6125-8997.
E-mail address: Ron.Pace@anu.edu.au (R.J. Pace).

0005-2728/$ - see front matter © 2004 Elsevier B.V. All rights reserved.
doi:10.1016/j.bbabio.2003.09.016

significant structural change (elongation of one of the Mn–Mn vectors by ~0.3 Å) seen on the $S_2 \rightarrow S_3$ transition. However, this oxo-radical could function as an H atom abstractor only on the $S_3 \rightarrow S_4 \rightarrow S_0$ step. Could this be sufficient? Two factors were acknowledged as pertinent:

(a) The observations at ANU by Wydrzynski et al. [8,9] that substrate water exchange with bulk occurred freely up to and including the S_3 state. This suggested that the catalytic site region might be in quasi-thermodynamic equilibrium with the solvent exterior so that electrostatic *lowering* of the pK_a of suitable groups (bound waters, hydroxyls, etc.), following electron removal, could be sufficient to mobilise protons on some S-state transitions. This point had been argued by Ahlbrink et al. [10].
(b) Reaction pathway computational studies by Siegbahn and Blomberg [11] on WOC model Mn systems. The favoured pathways, arrived at in these studies, involved reaction between a 'free' (or loosely bound) water molecule and an oxo-radical on Mn, with concerted proton transfer from the unbound water to a Mn hydroxo ligand as O—O bond formation develops.

Early in 2000, a version of the above ideas was submitted [12]. This also was challenged by the emergence soon after of the cyanobacterial PSII structure [5]. Here we reflect on a model also derived from the above considerations, but incorporating insights brought by the new X-ray structural data.

2. Catalytic core of the Mn/Ca site

At present, the PSII structure is not to atomic resolution. EXAFS and electron paramagnetic resonance (EPR) data are clear however that the Mn are magnetically coupled, at least pairwise, by μ-oxo and possibly μ-carboxylato bridges, with a characteristic Mn–Mn separation of ~2.7–2.8 Å in the pairs for the lower S-states [7]. One Ca is near (3.3–3.5 Å) to approximately two Mn [13].

There have been extensive efforts over the last two decades to mimic the water oxidising site of PSII. The majority of these have involved four Mn structures, on the expectation that the catalytic site is a tetranuclear complex. None of these compounds has exhibited water-splitting behaviour and only a couple have spectroscopic signatures even vaguely similar to the natural centre. However, synthetic (and natural) mixed valence Mn-dimers exhibit EPR spectra broadly similar to those seen in PSII. Further, the *only* synthetic Mn complex so far shown to display multiple turnover oxygen evolving activity is a dimer of Mn ions in high oxidation states [14]. Detailed modelling of the likely reaction mechanism in the natural system suggests that, no matter how many Mn may be present in total, only one pair of Mn and a Ca ion may be directly required for the water-splitting reaction [11,15].

The 'canonical' Mn derived EPR signal from the S_2 state is the so-called multiline signal (ML) [16]. This resembles spin 1/2 signals seen in mixed valence (III–IV or III–II) oxo-bridged Mn dimers, but contains more lines (~18–20). It has been modelled assuming four interacting Mn centres [17–19]. The ML signal, as conventionally generated for EPR study, may *not* always be a homogeneous species however [20–22]. It appears to consist, in some cases, of two overlapping signal types, a 'broad' and 'narrow' form, first inferred by Boussac from near infrared (NIR) turnover effects on the ML signal. Evans et al. [23] have shown that these forms have different low temperature storage stabilities and accessibility to small molecules. The narrow form is only ~130 mT wide with ~16 lines [22]. Remarkably, recent studies in our laboratories (Ahrling et al., BBA submitted) show that *both* of these forms functionally turnover in the first cycle, but that narrow form centres have converted to broad form by the second cycle (i.e. fifth flash in a series). This has important implications for the interpretation of EPR studies on the multiline signal, as typically generated. For example, the conditions used for the Mn electron nuclear double resonance (ENDOR) studies in Ref. [18] (i.e. ~1 M MeOH present in buffer), in our hands, produce roughly equimolar mixtures of both multiline types on the first cycle (i.e. one flash, etc.). This means that the Mn ENDOR seen may be from a *mixture* of centres, rather than from a homogeneous population of tetranuclear species. This matter requires further study.

The first and so far only multi-frequency simulation study of the ML signal (4, 9 and 35 GHz, [24]) assumed a mixed valence (III–IV) dimer model for the Mn cluster with unusual, anisotropic hyperfine parameters for *both* Mn spin centres. Nuclear quadrupole interactions (>60 MHz) found necessary to model the highly structured S-band spectrum [25] are almost certainly too large. These (and to date, all other) simulations are limited in assuming that the principal directions of all hyperfine interaction tensors on the anisotropic centres are co-incident. In low symmetry (e.g. protein) environments, this assumption will generally break down and additional parameters are needed relating all tensors to a common molecular frame. However, for conventional mixed valence Mn dimers, an important simplification almost *always* occurs. One centre, the Mn II (d^5) or Mn IV (d^3) is *not* subject to Jahn–Teller distortion and so has negligible quadrupole and near isotropic hyperfine interaction. Then the molecular frame is determined *solely* by the anisotropic (i.e. Mn III) partner. This appears always to obtain with successful simulations of Mn heterodimer EPR signals (model compound or protein centres, e.g. see Ref. [26]).

The other spin 1/2 multiline EPR signal seen from the functional Mn cluster occurs in the S_0 state, in the presence of non-inhibitory (~1 M) concentrations of MeOH [27,28]. This is even wider and more 'complex' than the S_2 ML, with ~22 lines, but the S_0 state contains one Mn II (see discussion in Ref. [12]). The (d^5) Mn II ion is particularly insensitive to ligand environment and Mn II

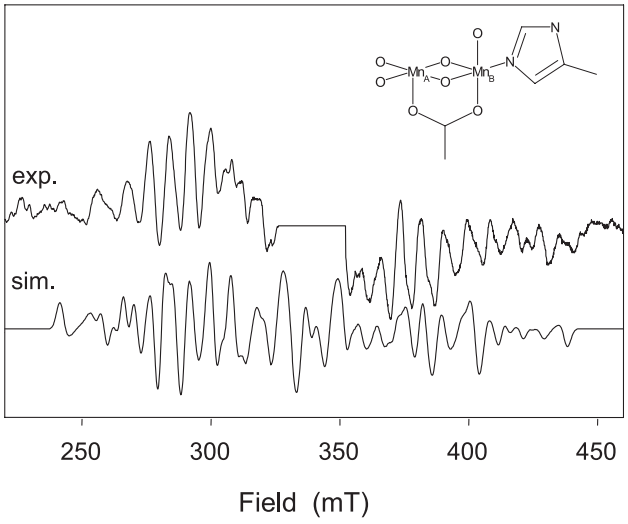

Fig. 1. Experimental S_0 state ML signal formed by flash turnover of plant PSII membrane samples containing ~ 1 M MeOH (from Ref. [28], see original reference for conditions, etc.). Simulated spectrum using a strong exchange Mn II–III dimer model (inset) and the following true ion parameter values: Mn_A (II); A_x, 268, A_y, 276, A_z 247, (A_{iso}) (264) MHz. Mn_B (III); A_x, 251, A_y, 340, A_z 172 (A_{iso}) (254) MHz. Q_x, −10.8, q_y, +7.2, q_z, +3.6 MHz. Molecule: g_x, 1.96, g_y, 1.98, g_z 2.03. Here $A_{x,y,z}$ are hyperfine and $q_{x,y,z}$ quadrupole component terms. $A_{(A)}$ (true ion) = 3/7 $A_{(A)}$ (fit), $A_{(B)}$ (true ion) = − 3/4 $A_{(B)}$ (fit) in the strong exchange limit [43]. Inset shows the dimer ligand environment previously inferred from S_2 state ML modelling [24].

hyperfine coupling is almost always isotropic, or near so. Fig. 1 shows that the S_0 multiline signal generated by flash turnover [28] is simulated by an anti-ferromagnetically coupled Mn II–III dimer (Fig. 1, inset), with ion parameters given in the figure legend. The Mn II centre (Mn_A) is typical (A_{ISO} ~ 260 MHz, see Ref. [18]) and near isotropic. The Mn III (Mn_B) however shows the pronounced rhombic asymmetry inferred earlier for the spin 3/2 centre in the S_2 ML simulations [24]. In the S_2 state this spin 3/2 centre could be a Mn IV, but is more likely a Mn III-(oxidised His), see Ref. [12]. The Mn III in S_0 has a substantial quadrupole asymmetry, but within physically reasonable bounds [18]. Another acknowledged spin 1/2 dimer signal from PSII, is the NO-induced multiline signal [29]. This is also a Mn II–III species, but weakly coupled, with substantially different single ion parameters to those in Fig. 1. It closely resembles an EPR signal from the dinuclear Mn (II–III) catalase, whose significance we return to below. Given these results and the *experimental* ambiguity attending the S_2 state ML signal(s), on which so much interpretation has rested, it now seems reasonable to explore possibilities in which only two Mn contribute significantly to the catalytic site function.

3. Substrate water exchange—mechanistic implications

Hillier and Wydrzynski [9] have studied the kinetics of substrate water exchange with the WOC in all stable S-states. The data are summarised in Table 1. A 'fast' and a 'slow' exchanging site are identified. We have shown previously [12] that the slow exchange kinetics are consistent with simple, unimolecular rate-determining steps, presumably breaking the metal–substrate ligand bond at the binding site. The fast exchange process is more consistent (at least in S_3) with restricted (single file) diffusion through a proteinaceous pore. These kinetics carry no 'memory' of the actual binding site, which must have substantially lower binding energy for substrate than the slow site, assuming both gain access to external water through the same channel. The inferred slow site bond energies ~ 70–90 kJ/mol, are compatible with H_2O/OH^- terminal ligation to a Mn III, but essentially exclude binding to Mn IV [12].

Vrettos et al. [30] have shown that Ca plays a specific, substrate-activating role in the WOC. Both its size and Lewis acidity are important. We assume, as have others [31,32], that one substrate water is bound to Ca (fast exchanging) and the other (slow exchanging) is bound to Mn. From Ref. [12], the latter is Mn III in the $S_{1,2,3}$ states. The data in Table 1 exhibit several interesting features;

(a) There is a 10^3-fold *decrease* in exchange rate from the slow site following the $S_0 \rightarrow S_1$ transition. This implies an increase in oxidation state of the relevant Mn ion and possibly also deprotonation ($H_2O \rightarrow OH^-$) of the bound substrate (transition is electroneutral [4]).
(b) The slow site exchange rate *increases* (~ 100-fold) on the $S_1 \rightarrow S_2$ transition and remains *unchanged* in S_3. This is completely counterintuitive, one anticipates a progressive *increase* in the magnitude of substrate binding energy through the S cycle as the mean redox level of the Mn cluster increases and protons are lost. However, the $S_1 \rightarrow S_2$ transition is electrogenic in fully intact PSII, involves no proton loss [4] and little change in the Mn cluster geometry [7], Thus internal proton *rearrangement* may cause the apparent substrate affinity change. This could be *reprotonation* of the OH^- which was deprotonated on $S_0 \rightarrow S_1$.
(c) On the $S_2 \rightarrow S_3$ transition, the fast site exchange rate slows down. This transition is nearly electroneutral [4],

Table 1
Substrate water exchange rates in WOC[a]

S-state	Slow		Fast	
	k_{ex} (10 °C, s^{-1})[b]	E_a (kJ/mol)[c]	k_{ex} (10 °C, s^{-1})[b]	E_a (kJ/mol)[c]
S_0	10–20[d]	–	>100	–
S_1	2.2×10^{-2}	86 ± 10	>100	–
S_2	2.2	75 ± 10[e]	>175	–
S_3	2.1	75 ± 10[e]	37 ± 2	~ 40 ± 5

[a] Data from Ref. [9].
[b] First-order exchange rate constant at 10 °C.
[c] Apparent activation energy.
[d] Range for $^{34}O_2$ and $^{36}O_2$ detected rates, see Ref. [9].
[e] Average for S_2 and S_3 combined data.

suggesting deprotonation of the substrate H_2O molecule at this low binding energy (Ca) site.

Combining all of the above yields the model shown in Fig. 2. This assumes that substrate/proton access to the catalytic region occurs through a single, restricted diffusion pathway, terminating at the metal binding sites. Mn_A, which is redox level II in S_0 and III in S_1 (see Fig. 1, inset) constitutes the slow exchange site and is at the 'end of the line'. A 'proton shuffle' between a bridge hydroxo and the substrate OH^- occurs in S_2, following oxidation centred near the other Mn (Mn_B). This restores the substrate form to be H_2O at the Mn_A site, reducing the binding energy. The purpose of the 'proton two-step' is twofold: (i) it converts the bridge to oxo-form, priming it for oxidation to an O radical in S_3, (ii) it sets the trigger for *back transfer* of an *H atom* in the $S_3 \rightarrow S_4 \rightarrow S_0$ step, which releases O_2. The latter is almost certainly a concerted process. It might involve electron transfer from the Ca bound OH^- to $Y_Z(ox)$, together with reaction of the resulting $OH^{\cdot}$ with the 'effective $OH^{\cdot}$' formed by (concerted) H abstraction from the Mn bound H_2O. Two observations lend credence to this: (i) the electron transfer rate to Y_Z on the $S_3 \rightarrow S_4 \rightarrow S_0$ transition is an order of magnitude *slower* than on the earlier S-state turnovers, all of which have similar $Y_Z(ox)$ reduction kinetics [33–35]. (ii) Of suitably sized di- and tri-valent cations which reconstitute into the Ca site, only the *weakest* Lewis acids (Ca, Sr) support water splitting [30]. Weak electrophiles are necessary if the bound OH^- is not to be rendered too stable against oxidation. The result is a transient formation of bound HOOH, which would rapidly oxidise through to O_2 plus $2H^+$. However, the key step is

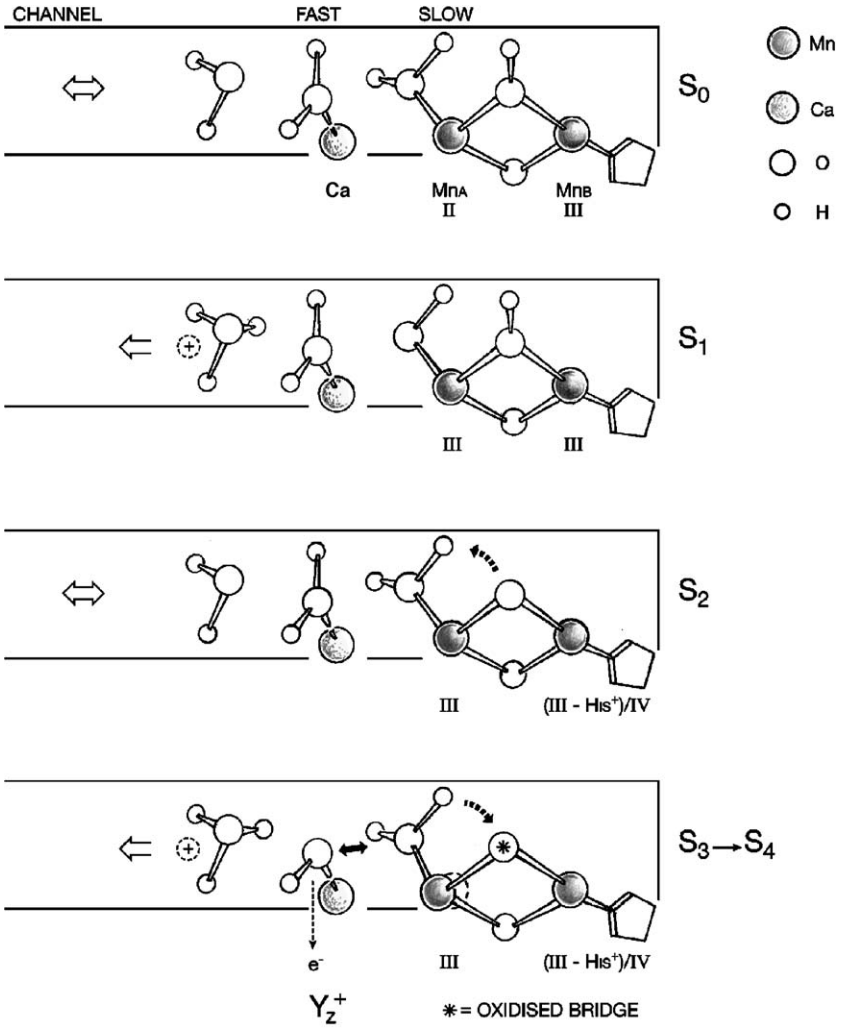

Fig. 2. Schematic representation of the water oxidising site in PSII, showing access to the fast and slow exchanging substrate binding sites through a common restricted water channel (see text). The proposed catalytic sequence and substrate protonation forms are indicated for each S-state. Back exchange of a proton from the bridge oxo (marked) to the tightly bound substrate hydroxyl occurs on the $S_1 \rightarrow S_2$ transition (as oxidation around Mn_B occurs), resulting in a lowering of the substrate affinity at Mn_A (see text and Table 1). The deprotonated bridge oxo becomes the O radical centre in S_3, to which H transfer occurs in the concerted O=O bond formation step ($S_3 \rightarrow S_4 \rightarrow S_0$). The low affinity site (Ca bound) water is possibly deprotonated in S_3 (electrostatic pK_a lowering), thus slowing the fast exchange rate (see text and Table 1). The high affinity water probably bridges between Mn_A and the Ca ion (see text and Fig. 3).

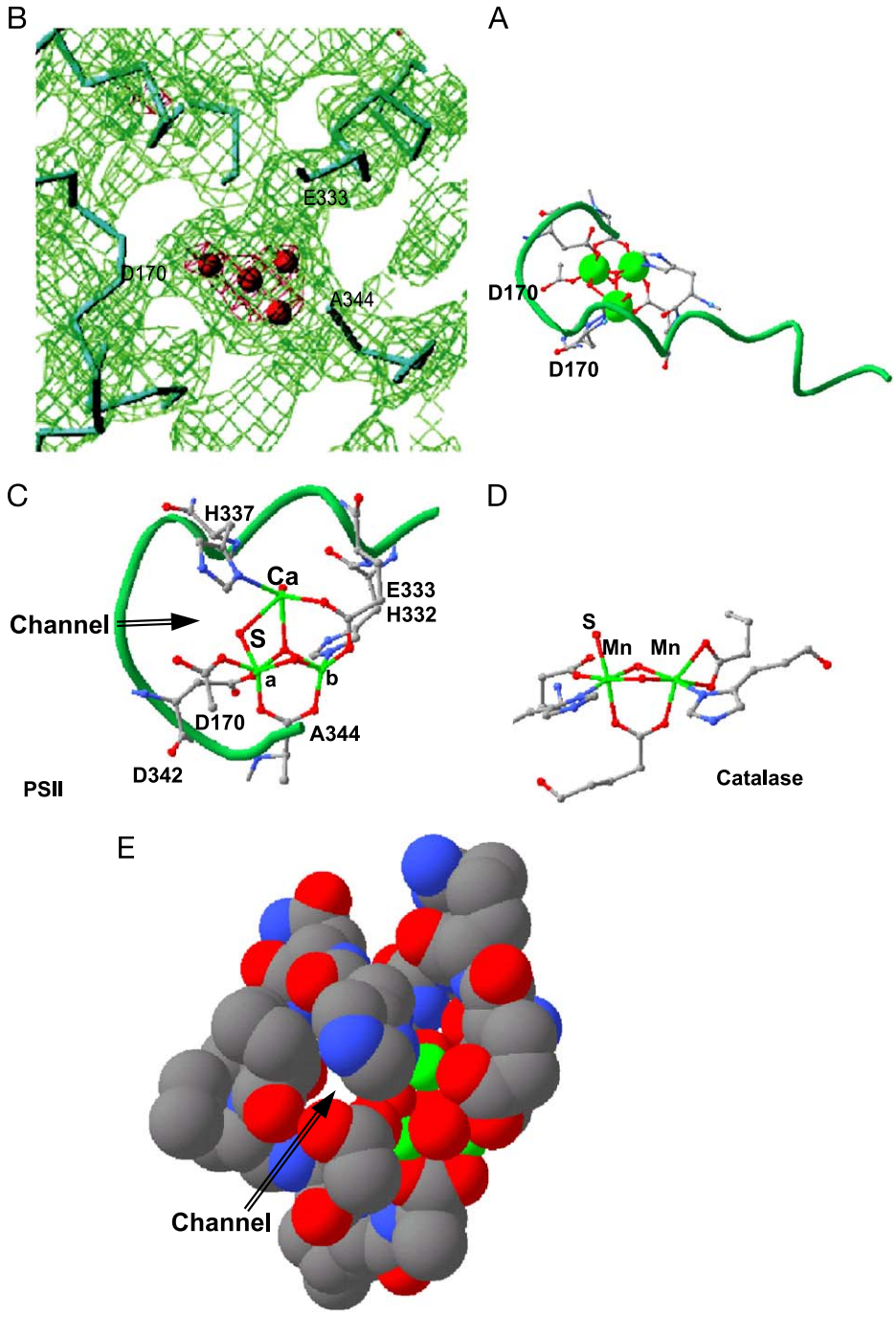

Fig. 3. (A) Molecular model, geometry optimised using Hyperchem software with AMBER94 parameter set, of the peptide chain folding for the last 20 residues of the D1 protein in PSII, containing a 2 Mn–1 Ca cluster, consistent with the data and arguments discussed here (see text). This is aligned to give best match with the 3.7 Å electron density map of the catalytic site region, given in Ref. [6] and reproduced in panel B (red 5.0σ, green 1.0σ contours). The suggested D170 ligation position, from the C-CD loop is shown. (C) Detail of the WOC metal cluster ligand geometry showing bound (slow) substrate (S) molecule (S_1 state). The low symmetry environment of Mn_B is evident. (D) Corresponding view of the oxidised dinuclear Mn active site in *L. plantarum* catalase, from Ref. [42] (substrate, S). In both cases, the substrate to be oxidised (shown as O in D) binds to a Mn III, along the axial direction, normal to the μ-oxo bridge plane. Electron transfer into the Mn cluster is facilitated by simultaneous proton transfer to a bridge oxo, which has been deprotonated on an earlier step. In PSII, the system is 'supercharged' by operating at a higher redox potential (with one to two oxidised ligands) and active positioning of the substrate molecules by Ca. (E) Space filling picture of the proposed WOC site from panel C. This shows a distinct channel (~ 3 Å diameter) leading to the active site region, which is weakly polar. The 5.0σ density cut-off (red) from panel B probably includes water molecules in this channel, as it captures the Mg centre from the accessory Chl_{D1} (upper left in picture). (Panel B) Copyright 2003, National Academy of Sciences, USA.

probably the H abstraction, as OH^- 'alone' has too high a single electron redox potential (~ 2 V) to be oxidised by Y_Z [36].

4. Protein site geometry

Mutagenesis studies on cyanobacterial PSII have identified only a few residues (six) that are likely candidates as ligands to Mn or Ca. All are on the D1 subunit and most (five) are near the C-terminus end of this peptide [37,38]. In fact, one is the terminal carboxylate. This region of the protein is conserved in all organisms that have been sequenced [39]. Such a small number is surprising and suggests spatially 'efficient' local folding of the peptide chain to contain the metal site.

In the metal cluster of the WOC, there is little evidence to support bridging by anything other than oxygen-derived species. The proposed Mn–Ca interaction at 3.3–3.5 Å is short and consistent only with oxo-bridging between Ca and (probably two) Mn [40]. The electron density volumes of the active site metal clusters seen in the cyanobacterial crystal structures are roughly triangular and 'flat' [5,6]. Since three points always define a plane, a simple solution is to have three metals (2 Mn–1 Ca) form an 'incomplete cubane', with oxo-carboxylato bridging. Fig. 3A shows an energy minimised structure of the last 20 residues of the D1 peptide C-terminus, aligned to give best fit with the published density map of Kamiya and Shen [6] (reproduced in Fig. 3B). This differs somewhat from the folding suggested by Kamiya and Shen, however, there appears to be no consensus structure at ~ 3.7 Å for the C-terminal region at present (see Ref. [41]). The peptide chain in our model is quasi-helical up to F339 and the last four residues 'wrap around' the cluster, providing ligation and defining a channel (Fig. 3C,E) to the active site. *All* residues suggested by mutagenesis ligate.

The active site geometry is shown in Fig. 3C, with a hydroxide bound between Mn_A and Ca. Recent water exchange measurements on Sr-substituted PSII suggest this as the likely slow site configuration (Hendry, Wydrzynski, submitted). Also, the suggested ligation direction of the D1, D170 carboxylate O is shown, which is consistent with the proposed location of this residue in both published PSII structures [6,41] (Fig. 3B). Mn_A has all O ligation and quasi-octahedral geometry, as inferred earlier from S_2 state ML modelling [24]. Mn_B contains the single His ligand (H332) and has low symmetry, as noted from the earlier EPR modelling and above. There is a distinct similarity between the WOC site and the dinuclear metal site in Mn catalase [42] (Fig. 3D). The WOC site is essentially 'catalase plus Ca', with the reducing substrates (H_2O and H_2O_2, respectively) similarly binding and undergoing H transfer to bridge oxo's, on O=O bond formation. In the catalase, this process is assisted by an adjacent glutamate residue (E178). It is interesting to speculate that D1 E189 may play the same role in the photosystem. This residue is believed to be part of a mechanistically important 'H bonding network', but not a ligand [38].

Acknowledgements

The authors are extremely grateful to Mr. Sam Hay for the energy minimisation of the peptide model and general assistance with Fig. 3.

References

[1] C.W. Hoganson, N. Lydakis-Simantiris, X.-S. Tang, C. Tommos, K. Warncke, G.T. Babcock, B.A. Diner, J. McCracken, S. Styring, A hydrogen-abstraction model for the function of Y_Z in photosynthetic oxygen evolution, Photosynthesis Research 46 (1995) 177–184.
[2] C.W. Hoganson, G.T. Babcock, A metalloradical mechanism for the generation of oxygen from water in photosynthesis, Science 277 (5334) (1997) 1953–1956.
[3] C. Tommos, G.T. Babcock, Oxygen production in nature: a light-driven metalloradical enzyme process, Accounts of Chemical Research 31 (1998) 18–25.
[4] F. Rappaport, M. Blanchard-Desce, J. Lavergne, Kinetics of electron transfer and electrochemical change during the redox transitions of the photosynthetic oxygen-evolving complex, Biochimica et Biophysica Acta 1184 (1994) 178–192.
[5] A. Zouni, H.T. Witt, J. Kern, P. Fromme, N. Krauss, W. Saenger, P. Orth, Crystal structure of photosystem II from *Synechococcus elongatus* at 3.8 Å resolution, Nature 409 (2001) 739–743.
[6] N. Kamiya, J.-R. Shen, Crystal structure of oxygen-evolving photosystem II from *Thermosynechococcus vulcanus* at 3.7 Å resolution, Proceedings of the National Academy of Sciences of the United States of America 100 (2003) 98–103.
[7] V.K. Yachandra, K. Sauer, M.P. Klein, Manganese cluster in photosynthesis: where plants oxidise water to dioxygen, Chemical Reviews 96 (1996) 2927–2950.
[8] J. Messinger, M. Badger, T. Wydrzynski, Detection of one slowly exchanging substrate water molecule in the S_3 state of photosystem II, Proceedings of the National Academy of Sciences of the United States of America 92 (1995) 3209–3213.
[9] W. Hillier, T. Wydrzynski, Oxygen ligand exchange at metal sites—implications for the O_2 evolving mechanism of photosystem II, Biochimica et Biophysica Acta 1503 (2001) 197–209.
[10] R. Ahlbrink, M. Haumann, D. Cherepanov, O. Bögerhausen, A. Mulkidjanian, W. Junge, Function of tyrosine Z in water oxidation by photosystem II: electrostatical promotor instead of hydrogen abstractor, Biochemistry 37 (1998) 1131–1142.
[11] P.E.M. Siegbahn, M.R.A. Blomberg, Density functional theory of biologically relevant metal centres, Annual Review of Physical Chemistry 50 (1999) 221–249.
[12] D. Kuzek, R.J. Pace, Probing the Mn oxidation states in the OEC. Insights from spectroscopic, computational and kinetic data, Biochimica et Biophysica Acta 1503 (2001) 123–137.
[13] R.M. Cinco, J.H. Robblee, A. Rompel, C. Fernandez, V.K. Yachandra, K. Sauer, M.P. Klein, Strontium EXAFS reveals the proximity of calcium to the manganese cluster of oxygen evolving photosytem II, Journal of Physical Chemistry B 102 (1998) 8248–8256.
[14] J. Limburg, J.S. Vrettos, H. Chen, J.C. de Paula, R.H. Crabtree, G.W. Brudvig, Characterization of the O_2-evolving reaction catalyzed by [(terpy)(H_2O)MnIII(O)2MnIV(OH_2)(terpy)](NO_3)3 (terpy = 2,2′ : 6,2″-terpyridine), Journal of the American Chemical Society 123 (2001) 423–430.

[15] J.S. Vrettos, J. Limburg, G.W. Brudvig, Mechanism of photosynthetic water oxidation: combining biophysical studies of photosystem II with inorganic model chemistry, Biochimica et Biophysica Acta 1503 (2001) 229–245.
[16] G.C. Dismukes, Y. Siderer, Intermediates of a polynuclear manganese center involved in photosynthetic oxidation of water, Proceedings of the National Academy of Sciences of the United States of America 78 (1981) 274–278.
[17] K. Hasegawa, M. Kusunoki, Y. Inoue, T.-A. Ono, Simulation of the S2-state multiline EPR signal in oriented photosystem II membranes: structural implications for the manganese cluster in an oxygen-evolving complex, Biochemistry 37 (1998) 9457–9465.
[18] J.M. Peloquin, K.A. Campbell, D.W. Randall, M.A. Evanchik, V.L. Pecoraro, W.H. Armstrong, D.R. Britt, ^{55}Mn pulsed ENDOR of the S2-state multiline EPR signal of photosytem II: implications on the structure of the tetranuclear Mn cluster, Journal of the American Chemical Society 122 (2000) 10926–10942.
[19] M. Zheng, G.C. Dismukes, Orbital configuration of the valence electrons, ligand field symmetry and manganese oxidation states of the photosynthetic water oxidizing complex: analysis of the S2 state multiline EPR signals, Inorganic Chemistry 35 (1996) 3307–3319.
[20] J.C. de Paula, G.W. Brudvig, Magnetic properties of manganese in photosynthetic O_2-evolving complex, Journal of the American Chemical Society 107 (1985) 2643–2648.
[21] A. Boussac, Inhomogeneity of the EPR multiline signal from the S_2-state of the photosystem II oxygen evolving enzyme, Journal of Bioinorganic Chemistry 2 (1997) 580–585.
[22] M.C.W. Evans, A.M. Rich, J.H.A. Nugent, Evidence for the presence of a component of the Mn complex of the photosystem II reaction centre which is exposed to water in the S2 state of the water oxidation complex, FEBS Letters 477 (2000) 113–117.
[23] M.C.W. Evans, K. Gourovskaya, J.H.A. Nugent, Investigation of the interaction of the water oxidising manganese complex of photosystem II with the aqueous solvent environment, FEBS Letters 450 (1999) 285–288.
[24] K.A. Åhrling, R.J. Pace, Simulation of the S_2 state multiline electron paramagnetic resonance signal of photosystem II: a multifrequency approach, Biophysical Journal 68 (1995) 2081–2090.
[25] A. Haddy, R. Aasa, Ö. Hansson, S-band EPR studies of the S_2-state multiline signal from the photosynthetic oxygen-evolving complex, Biochemistry 28 (1989) 6954–6959.
[26] K.-O. Schafer, R. Bittl, W. Zweygart, F. Lendzian, G. Haselhorst, T. Weyhermuller, K. Wieghardt, W. Lubitz, Electronic structure of antiferromagnetically coupled dinuclear manganese (MnIII MnIV) complexes studies by magnetic resonance techniques, Journal of the American Chemical Society 120 (50) (1998) 13104–13120.
[27] J. Messinger, J.H.A. Nugent, M.C.W. Evans, Detection of an EPR multiline signal for the S_0* state in photosystem II, Biochemistry 36 (1997) 11055–11060.
[28] K.A. Åhrling, S. Peterson, S. Styring, An oscillating manganese electron paramagnetic resonance signal from the S_0 state of the oxygen evolving complex in photosystem II, Biochemistry 36 (43) (1997) 13148–13152.
[29] J. Sarrou, N. Ioannidis, Y. Deligiannakis, V. Petrouleas, A Mn(II)–Mn(III) EPR signal arises from the interaction of NO with the S1 state of the water-oxidizing complex of photosystem II, Biochemistry 37 (1998) 3581–33587.
[30] J.S. Vrettos, D.A. Stone, G.W. Brudvig, Quantifying the ion selectivity of the Ca^{2+} site in photosystem II: evidence for direct involvement of Ca^{2+} in O_2 formation, Biochemistry 40 (2001) 7937–7945.
[31] A.W. Rutherford, J.L. Zimmermann, A. Boussac, Oxygen evolution, in: J. Barber (Ed.), The Photosystems: Structure, Function and Molecular Biology, Elsevier, Dordrecht, 1992, pp. 179–229.
[32] J. Limburg, V.A. Szalai, G.W. Brudvig, A mechanistic and structural model for the formation and reactivity of a MnV═O species in photosynthetic water oxidation, Journal of the Chemical Society. Dalton Transactions, (1999) 1353–1361.
[33] G.T. Babcock, R.E. Blankenship, K. Sauer, Reaction kinetics for positive charge accumulation on the water side of chloroplast photosystem II, FEBS Letters 61 (1976) 286–289.
[34] M.R. Razeghifard, C. Klughammer, R.J. Pace, Electron paramagnetic resonance kinetic studies of the S states in spinach thylakoids, Biochemistry 36 (1997) 86–92.
[35] M.R. Razeghifard, R.J. Pace, Electron paramagnetic resonance kinetic studies of the S states in spinach PSII membranes, Biochimica et Biophysica Acta 1322 (1997) 141–150.
[36] K. Yamaguchi, D.T. Sawyer, Redox chemistry for the mononuclear Tris(picolinato)-, Tris(acetylacetonato)-, and Tris(8-quinolinato)manganese(III) complexes: reaction mimics for the water-oxidation cofactor in photosystem II, Inorganic Chemistry 24 (1985) 971–976.
[37] B.A. Diner, Amino acid residues involved in the coordination and assembly of the manganese cluster of photosystem II. Proton-coupled electron transport of the redox-active tyrosines and its realationship to water oxidation, Biochimica et Biophysica Acta 1503 (2001) 147–163.
[38] R.J. Debus, Amino acid residues that modulate the properties of tyrosine Y_Z and the manganese cluster in the water oxidising complex of Photosystem II, Biochimica et Biophysica Acta 1503 (2001) 164–186.
[39] B. Svensson, I. Vass, S. Styring, Sequence analysis of the D1 and D2 reaction center proteins of photosystem II, Zeitschrift für Naturforschung 46c (1991) 765–776.
[40] P. Hubberstey, Elements of group 2, Coordination Chemistry Reviews 56 (1984) 78–112.
[41] A. Zouni, J. Kern, B. Loll, P. Fromme, H. Witt, P. Orth, N. Krauss, W. Saenger, J. Biesiadka, Biochemical characterisation and crystal structure of water oxidising Photosystem II from *Synechococcus elongatus*, in: Proceedings of the 12th International Congress on Photosynthesis, vol. S05-003. CSIRO Publishing, Collingwood, Australia, 2002, pp. 1–6.
[42] V.V. Barynin, M.M. Whittaker, S.V. Antonyuk, V.S. Lamzin, P.M. Harrison, P.J. Artymiuk, J.W. Whittaker, Crystal structure of manganese catalase from *Lactobacillus plantarum*, Structure 9 (2001) 725–738.
[43] A. Bencini, D. Gatteschi, Electron Paramagnetic Resonance of Exchange Coupled Systems, 1st ed., Springer-Verlag, Berlin, 1990, 300 pp.